Range-based Scan Matching for LiDAR-SLAM with Non-repetitive Omnidirectional LiDAR

Masafumi N.[1*], Kenshiro Y.[1], Tetsu Y.[1], Nobuaki K.[2], Etsuro S.[2]

[1]Shibaura Institute of Technology, Japan

[2]Tokyo University of Marine Science and Technology, Japan

*mnaka@shibaura-it.ac.jp

***Abstract*:** *Three-dimensional light detection and ranging (3D-LiDAR) systems are widely used for simultaneous localization and mapping (SLAM) and object recognition. Conventional systems use repetitive horizontal scanning LiDAR to provide dense point clouds, however, they have measurement limitations due to narrow vertical fields-of-view (FOVs). These limitations are often addressed by combining multiple sensors or using mechanical rotation. Repetitive LiDARs can provide high temporal scan overlap, which is suitable for iterative closest point (ICP)-based scan matching. By contrast, non-repetitive LiDARs use micro-electromechanical system mirrors to achieve wide FOV coverage with high angular resolution. They reduce sensor requirements and eliminate the need for mechanical rotation. However, there is little overlap between adjacent scans, thus, conventional ICP methodologies are less effective. Therefore, we propose a range-based scan-matching methodology designed for non-repetitive LiDAR. First, LiDAR scans are rasterized into range images defined by horizontal and vertical scan angles. Reference scans are then projected into this space after rigid transformations, and alignment is evaluated using image subtraction processing. The processing accelerates scan matching by replacing the inefficient voxel-based point cloud matching with a simpler 1-D depth minimization task. Moreover, a fast point cloud rasterizer is applied to generate the range images. We conducted experiments using an autonomous boat, Raicho I, which is equipped with a non-repetitive omnidirectional LiDAR (Livox MID-360) as well as conventional Velodyne LiDARs for a comparison experiment. We selected Kanda and Nihonbashi Rivers in Tokyo, which included GNSS and non-GNSS environments. Through these experiments, we evaluated the accuracy of point cloud integration and the processing speed of our proposed methodology.*

Keywords: *LiDAR-SLAM, scan matching, omnidirectional LiDAR, autonomous boat*

Introduction

There are two main types of 3-D LiDAR for wide area measurement. The first type is a horizontally scanning LiDAR that performs repetitive linear scans. To achieve uniform spatial resolution for LiDAR-SLAM applications, either multiple LiDAR sensors are often combined, or the LiDAR itself is physically rotated. Conventional LiDAR-SLAM techniques typically rely on repetitive-scanning LiDAR and apply scan-matching algorithms, such as the iterative closest point (ICP) methodology, to align sequential scan lines. These methodologies benefit from the presence of numerous candidate

correspondences between adjacent scans and use point-to-point, point-to-line, or point-to-plane matching strategies.

The second type is a LiDAR with non-repetitive and nonhorizontal scan lines using micro-electromechanical system mirrors (Wang, et al., 2020) to enable the acquisition of wide field-of-view (FOV) point clouds. Repetitive-scanning LiDAR can capture high-resolution data across a wide horizontal range, however, it is limited by a narrow vertical FOV and low vertical angular resolution. Although it requires a longer acquisition time, a non-repetitive LiDAR achieves high angular resolution in both the horizontal and vertical directions (Aijazi, et al., 2024). Consequently, a non-repetitive LiDAR can reduce the number of 3D-LiDAR units needed and eliminate the need for rotational mechanisms when capturing wide-area point clouds. However, conventional scan-matching techniques are less effective for SLAM with non-repetitive LiDARs because the adjacent scans have little overlap. Existing approaches address this limitation by incorporating motion distortion correction with inertial measurement units for tightly coupled position and attitude estimation. These approaches also use scan matching via point-to-plane methodology based on multiple surface normal vectors (Gao, et al., 2024). In addition, scan-to-map alignment registers local scans with global 3-D maps. This study investigates the use of a non-repetitive and omnidirectional LiDAR for SLAM applications to develop a more compact and efficient LiDAR-SLAM system.

We propose a range-based point-to-point scan-matching methodology suitable for non-repetitive omnidirectional LiDAR to enable robust SLAM processing in environments lacking planar surfaces. We verify the feasibility of the proposed methodology using data acquired from a non-repetitive omnidirectional LiDAR mounted on a boat through laser scanning experiments conducted in urban river environments.

Methodology

We proposed a range-based scan-matching methodology, for LiDAR-SLAM as shown in Figure 1. The range-based scan matching is based on rigid transformations between scenes as well as conventional LiDAR-SLAM. The conventional LiDAR-SLAM is processed in a voxel space, whereas the range-based scan matching is processed with the FOV from a LiDAR. In range-based scan matching, the base scene of the LiDAR scan data is first rasterized onto a FOV space with the horizontal and vertical angles as the respective axes. The resolution of the range image is determined by the scan angle resolution of the LiDAR.

Next, the reference scene of the LiDAR scan data is back-projected onto the same FOV space after a rotation and translation transformation that minimizes the relative distances between the point clouds of the base and reference scenes. Image subtraction is used to evaluate the distances between the base and reference range images of the point clouds so that the closest point search problem transforms into an image subtraction problem.

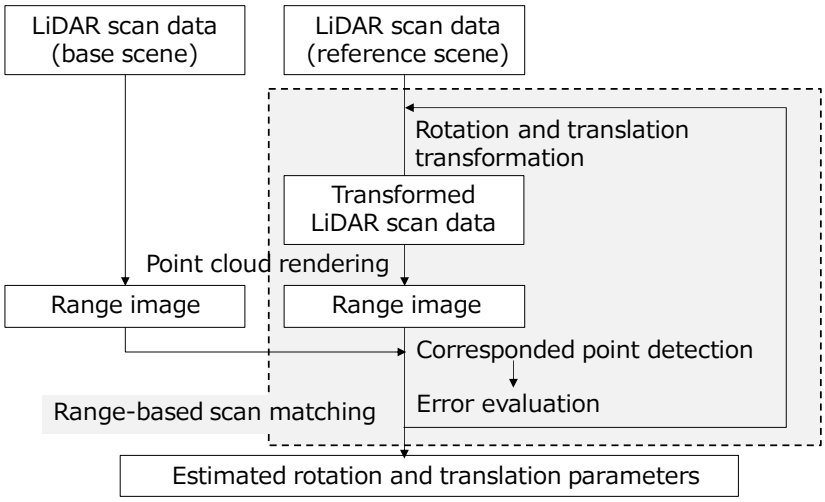

Figure 1: Proposed Methodology.

This process reduces the computational load by simplifying the 3-D distance minimization into the 1-D distance (depth) minimization between the base and reference point clouds. It also speeds up the search for neighboring points by referencing them directly, thereby eliminating the processing of the closest point search which is a technical issue of the ICP algorithm. This process also avoids the issue of voxel space bloating when searching for the closest points in voxel space for point clouds measured over a wide area. Furthermore, the process improves processing efficiency when working with point clouds with few corresponding points compared with the nearest neighbor search using kd-trees. However, our methodology requires repeatedly generating range images due to the extensive search for the rotation and translation parameters of the reference point clouds. Therefore, the range image generation process is a bottleneck step in our proposed methodology. Nevertheless, we apply a rapid rasterizer that geometrically simulates point cloud self-occlusion (Nakagawa et al., 2014) to speed up the overall processing.

Figure 2 shows an example of range-based scan matching. It illustrates the point cloud of the reference scene projected onto the FOV space after rotation and translation (Figure 2a), the point cloud of the reference scene projected onto the FOV space after rotation and translation (Figure 2b), and the extracted neighboring point clouds after superimposing them (Figure 2c).

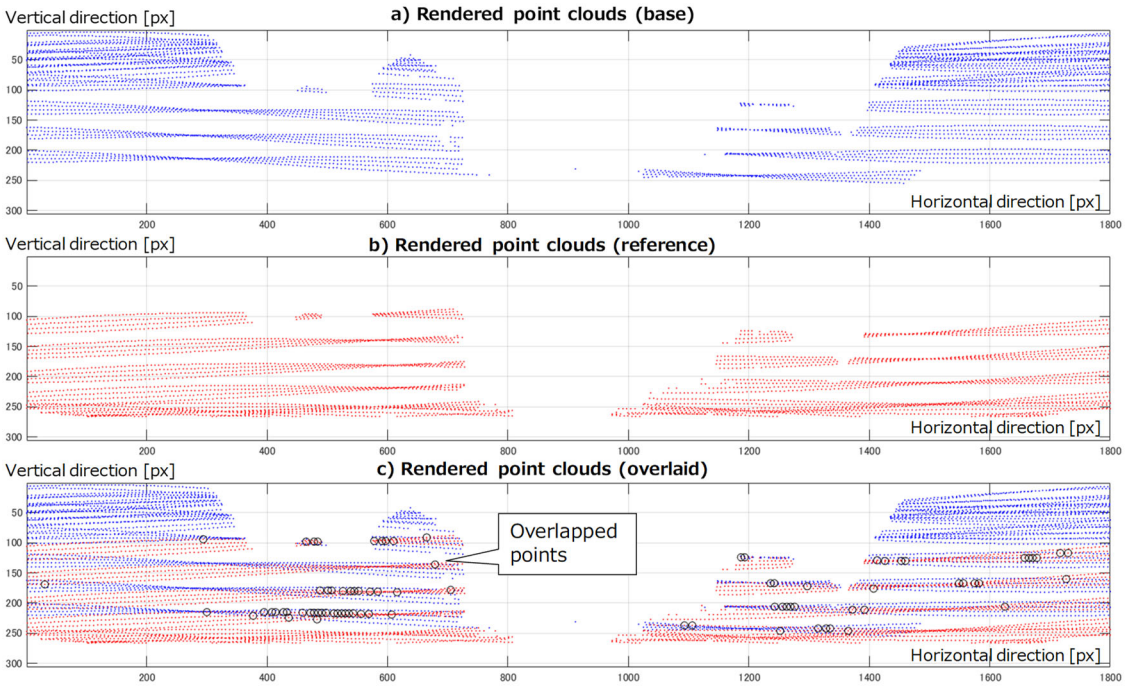

Figure 2: Part of Range-based Scan Matching.

Experiments

We selected the Kanda and Nihonbashi River in Tokyo as the sites for our experiments. The experiments were conducted on September 30, 2024. As shown in Figure 3, the experimental sites included water surfaces, revetments, bridges, buildings, vegetation, and other boats. Although areas under bridges and surrounded by dense buildings exist, the Kanda River is basically a GNSS environment. In contrast, the Nihonbashi River is a non-GNSS environment located under an expressway running alongside the river. The environmental conditions included calm weather with minor surface reflections.

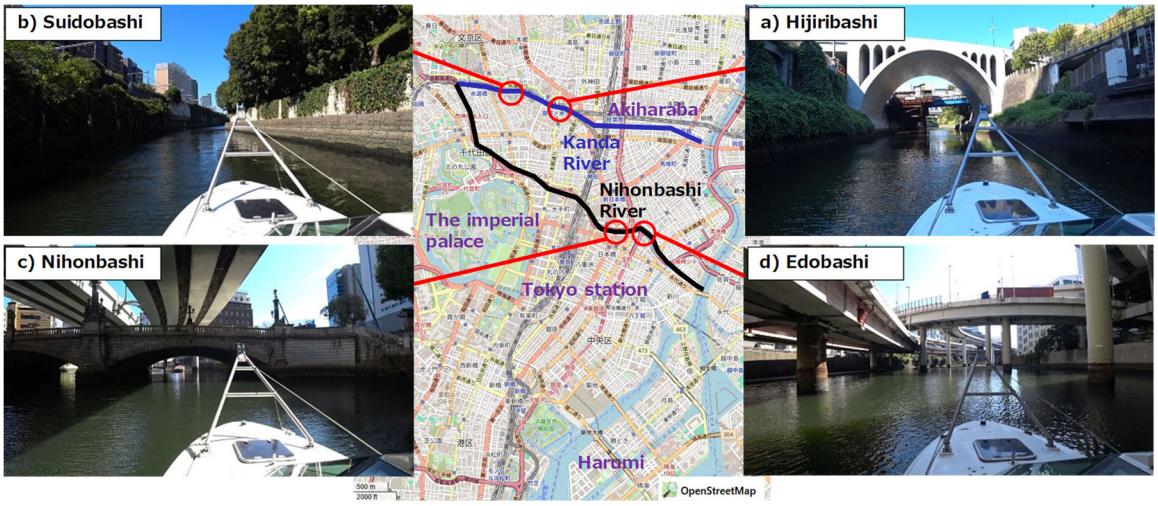

Figure 3: Experimental Sites.

For 3-D measurements, we also selected a waterborne mobile mapping system (MMS) (Nakagawa, et al., 2024), which consists of LiDARs and GNSS devices mounted on a 10-meter-long, battery-powered, autonomous boat called as Raicho I, as shown in Figure 4. We used two types of LiDARs. The first type of LiDAR was a non-repetitive omnidirectional LiDAR (MID-360, Livox). The sensor provides a horizontal FOV of 360° and a vertical FOV of 59°, producing approximately 100,000 points per second. The boat traveled at speeds of 4–6 knots, enabling stable data acquisition in various environments, including narrow and shallow waterways. The second type of LiDAR was a repetitive-scanning LiDAR for acquiring reference data. For the experiment, we used a horizontal scanning LiDAR (VLP32-C, Velodyne) and an oblique scanning LiDAR (VLP16, Velodyne), and GNSS with centimeter-level augmentation services to compare with the non- repetitive LiDAR. These LiDARs were mounted on the roof deck of the boat. At a navigation speed of 4 to 6 knots, we acquired LiDAR point clouds with 720,000 frames in LVX2 (non- repetitive LiDAR) and PCAP (repetitive-scanning LiDAR) formats over approximately 7,200 seconds. We selected several sections of the one-way route and processed each section at 1,200 frames. For range-based scan matching, the rendering angle resolution for the closest point searching was set to 0.2° for each section. Furthermore, we evaluated computational performance using the acquired point clouds. These experiments were conducted on a laptop PC with an Intel Core Ultra 7 CPU (3.80 GHz) and 32 GB of RAM. The implementation was written in MATLAB. Baseline comparisons included an ICP-based scan-matching implementation.

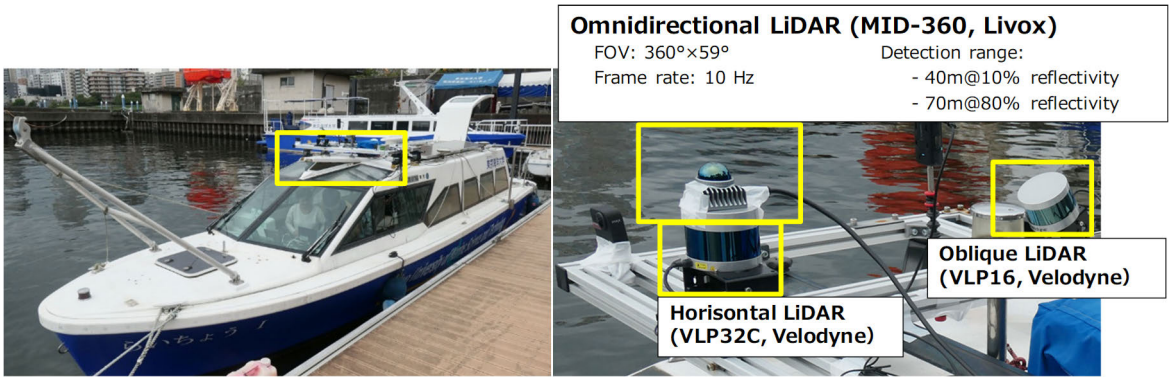

Figure 4: Waterborne MMS.

Results and Discussion

Figure 5 shows the estimated trajectories and the integrated point clouds, which are visualized in the horizontal sections of each scene. Red lines indicate estimated trajectories,

and blue points indicate integrated point clouds. Moreover, the scan-matching accuracy was approximately 3 cm in each scan matching. Furthermore, the geometry of objects, such as revetments, bridges, piers, and vegetation, can be clearly recognized. Based on these results, we confirmed that the poses of the moving LiDAR were accurately estimated in the range-based scan matching.

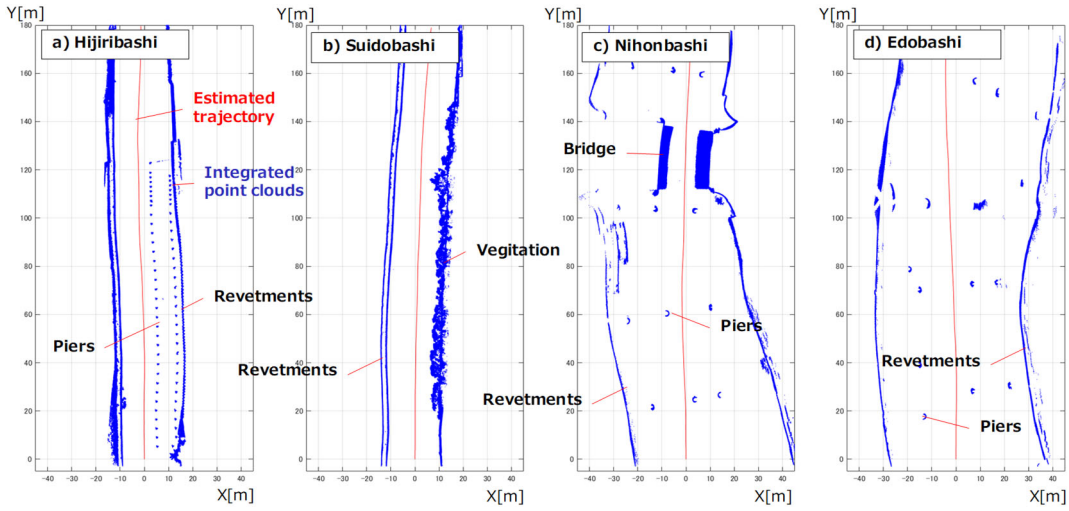

Figure 5: Estimated Trajectories and Integrated Point Clouds.

Figure 6 shows the integrated point clouds, which are visualized in the 3-D space of each scene with point density ranging from 5 cm to 10 cm and adjusted LiDAR intensity values. The results indicate that objects, such as revetments, bridges, and vegetation were clearly reconstructed because the poses of the moving LiDAR were accurately estimated in the range-based scan matching.

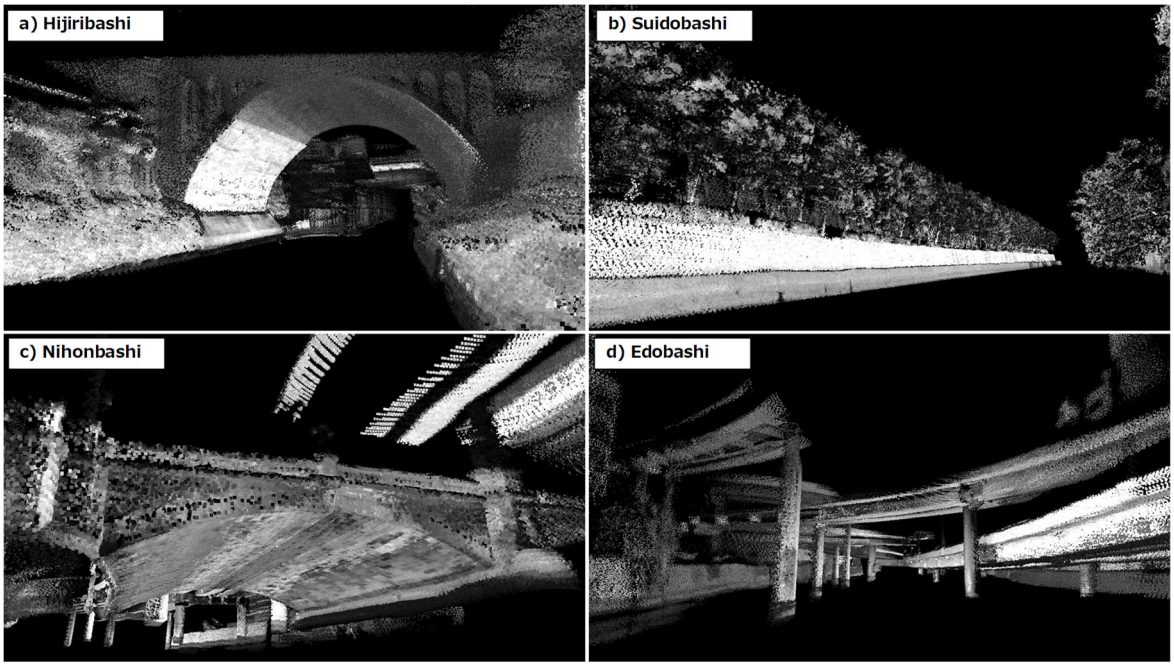

Figure 6: Integrated Point Clouds.

Table 1 shows the processing time for LiDAR-SLAM in each scene, including range-image-based matching and point cloud integration. In the experiment, acquiring LiDAR data at rate of 10 Hz took 120 seconds for 1,200 frames. Moreover, the processing time for each scene was less than 120 seconds during LiDAR data acquisition. Therefore, as shown in Table 1, the proposed methodology enabled LiDAR-SLAM processing within a practical timeframe.

Table 1: LiDAR-SLAM Processing Parameters and Processing Time.

Evaluated sections	The number of frames	Rendering angle resolution for near-point searching	Prosessing time [s]
a) Hijiribashi (Kanda River)	1200	0.2°	376.6
b) Suidobashi (Kanda River)	1200	0.2°	340.7
c) Nihonbashi (Nihonbashi River)	1200	0.2°	341.2
d) Edobashi (Nihonbashi River)	1200	0.2°	339.7

Figure 7 shows comparisons of integrated point clouds, processed with the same LiDAR-SLAM program, using both non- repetitive and repetitive LiDAR scanning data. Figures 6a and 6c show the results of processing non-repetitive LiDAR data. Figures 6b and 6d show the results of processing repetitive LiDAR data. As shown in the figures, Figures 6b and 6d are clearer than Figures 6a and 6c. This result suggests that the pose estimation using repetitive LiDAR data is more accurate than pose estimation using non- repetitive LiDAR data, because the former involves processing a greater number of corresponding points.

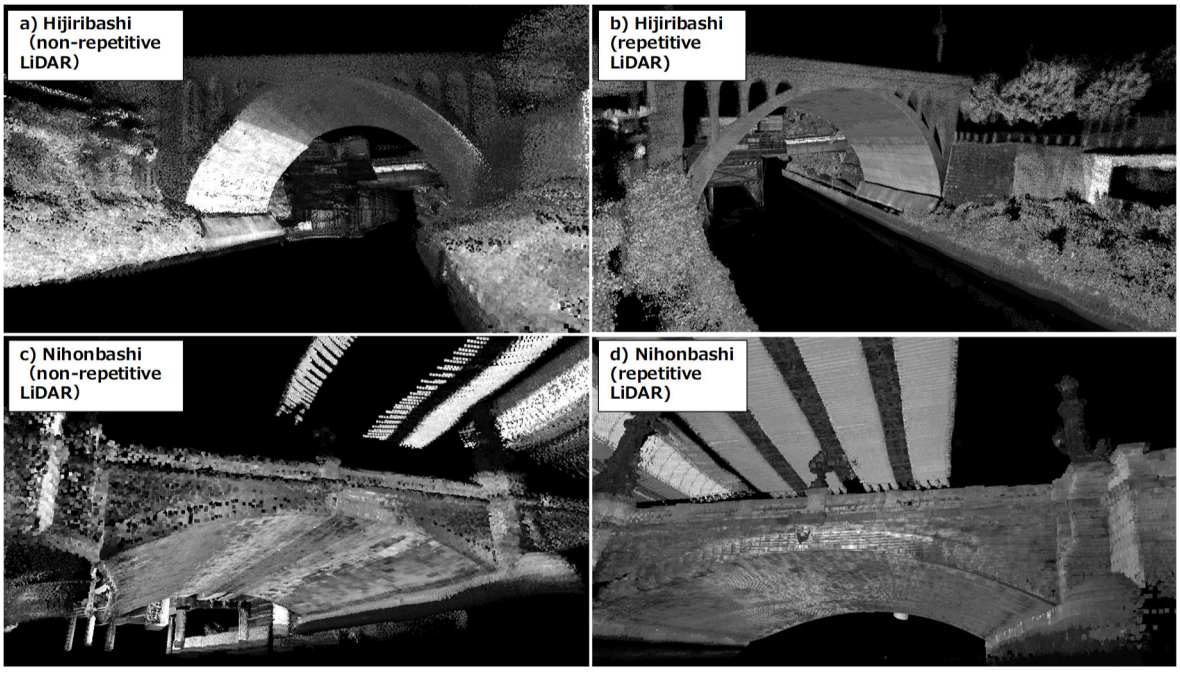

Figure 7: Comparisons of Integrated Point Clouds.

Figure 8 (a) shows an example of angle estimation results in 1-D visualization of a 3-D direction (roll, pitch and yaw). As shown in the figure, peaks can be easily formed even in areas consisting of straight and parallel revetments. By contrast, Figure 8 (b) shows an example of the results of translation estimation in 1-D visualization of a 3D- position (X, Y, and Z). As shown in the figure, peaks are hard to form in these areas.

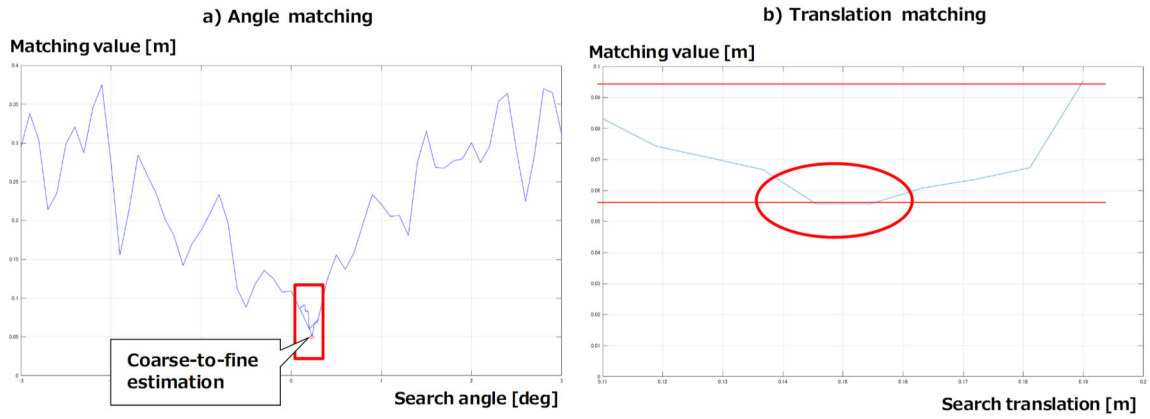

Figure 8: Examples of Pose Estimation Results in River Environments.

Conclusion

In this study, we developed a scan-matching methodology for non-repetitive omnidirectional LiDARs. Although conventional repetitive systems have the advantage of corresponding temporal scan data for ICP-based alignment, their FOV is limited so that multiple sensors or mechanical rotation systems are required. Therefore, we focused on non-repetitive and omnidirectional LiDARs to acquire high-resolution point clouds using a single LiDAR. Although non-repetitive LiDAR reduces system complexity, the lack of temporal scan data overlap renders conventional scan-matching unreliable. To address this issue, we developed a range-based point-to-point scan matching methodology. We evaluated our proposed methodology through experiments conducted in urban rivers using non-repetitive and repetitive LiDARs mounted on a waterborne MMS. The results showed stable trajectory estimation and clear reconstruction of objects, such as revetments, bridges, and vegetation, with an accuracy of approximately 3 cm per scan. Moreover, real-time processing was achieved through a simpler 1-D depth minimization task and a fast point cloud rasterizer. Based on these results, we confirmed that our proposed methodology using non-repetitive LiDARs performs robustly with real-time processing, demonstrating its potential for compact and efficient SLAM systems.

Acknowledgements

This study was supported by JSPS KAKENHI Grant Number JP24K07704 and Shibaura Institute of Technology Inter-University Collaboration Research Grant (724MA58292).

References

Aijazi, A. K., Checchin, P., (2024). Non-Repetitive Scanning LiDAR Sensor for Robust 3D Point Cloud Registration in Localization and Mapping Applications. Sensors, 24(2), 378.

Gao, Y., Zhao, L., (2024). VE-LIOM: A Versatile and Efficient LiDAR-Inertial Odometry and Mapping System, Remote Sensing, 16(15), 2772.

Nakagawa, M., Yamamoto, T., Kataoka, K., Shiozaki, M., Ohhashi, T., (2014). A Point-based Rendering for 3D Polygon Extraction In Indoor Environment, The 35th Asian Conference on Remote Sensing 2014, 6 pages.

Nakagawa, M., Kimura, N., Sadachika, N., Komori, T., Kubo, N., Shimizu, E., (2024). Streaming Point Cloud Segmentation of GNSS/SLAM-LiDAR and Multi-beam Scanning Sonar Data for Urban River Mapping, The 45th Asian Conference on Remote Sensing 2024, 19 pages.

Wang, D., Watkins, C., Xie, H., (2020). MEMS Mirrors for LiDAR: A Review. Micromachines, 11(5), 456.